Research Article

Cancer Immunology Research

LncRNA-MM2P Identified as a Modulator of Macrophage M2 Polarization

Ji Cao[1], Rong Dong[1,2], Li Jiang[1], Yanling Gong[1], Meng Yuan[1], Jieqiong You[1], Wen Meng[2], Zhanlei Chen[3], Ning Zhang[4], Qinjie Weng[1], Hong Zhu[1], Qiaojun He[1], Meidan Ying[1], and Bo Yang[1]

Abstract

M2 polarization of macrophages is essential for their function in immunologic tolerance, which might promote tumorigenesis. However, the molecular mechanism behind the polarization process is not fully understood. Given that several lines of evidence have suggested that long noncoding RNAs (lncRNAs) could be involved in regulating immune cell differentiation and function, the current study aimed to identify the lncRNAs that specifically modulate M2 macrophage polarization. By utilizing a series of cell-based M2 macrophage polarization models, a total of 25 lncRNAs with altered expression were documented based on lncRNA microarray-based profiling assays. Among them, lncRNA-MM2P was the only lncRNA upregulated during M2 polarization but downregulated in M1 macrophages. Knockdown of lncRNA-MM2P blocked cytokine-driven M2 polarization of macrophages and weakened the angiogenesis-promoting feature of M2 macrophages by reducing phosphorylation on STAT6. Moreover, manipulating lncRNA-MM2P in macrophages impaired macrophage-mediated promotion of tumorigenesis, tumor growth *in vivo*, and tumor angiogenesis. Collectively, our study identifies lncRNA-MM2P as a modulator required for macrophage M2 polarization and uncovers its role in macrophage-promoted tumorigenesis.

Introduction

Tumors are composed not only of cancer cells but also of an array of stromal cells such as tumor-associated macrophages (TAMs), which might regulate tumor growth and progression, angiogenesis, and adaptive immunity (1). So far, two major functional types of macrophages have been identified. Macrophages that promote the Th1-type inflammatory response and have microbicidal and tumoricidal activity are called M1 macrophages (also known as classically activated macrophages). M2 macrophages (also known as alternatively activated macrophages) are immunologic modulators that have little microbiocidal activity, can reside and proliferate in tissues, and support Th2-mediated disease, homeostasis, and thermogenesis (2–4). Although both M1 and M2 macrophages have been observed in tumors, evidence suggests that M2 macrophages are the predominant subtype found in tumors and that they tend to promote tumor progression (5, 6). Several groups, including ours, have reported that both interruption of the cross-talk between TAMs and tumor cells and suppression of macrophage M2 polarization can prevent tumorigenesis and metastasis (7–10).

Although several transcription factors, such as Signal Transducer and Activator of Transcription (STAT) and CCAAT/Enhancer Binding Proteins β (C/EBPβ), that are directly or indirectly activated by certain cytokines have been identified as playing roles in the M2 polarization of macrophages, the molecular mechanism underlying M2 polarization remains unclear (11). Evidence has indicated that long noncoding RNAs (lncRNA) regulate many cellular and developmental processes, including cell proliferation, apoptosis, and differentiation (12–14). Aberrant expression of lncRNAs is associated with the progression of pathophysiologic conditions including diabetes, cancer, tissue fibrosis, and cardiovascular disease (15–17). Although efforts have been directed at understanding the mechanism of lncRNAs in regulating gene expression (18, 19), little progress has been achieved in characterizing the functional lncRNAs dictating macrophage M2 polarization.

In the current study, we used a lncRNA microarray-based profiling assay to document changes in the abundance of lncRNAs polarized by IL13 in the RAW264.7 cell line and bone marrow–derived macrophages (BMDM). By examining different macrophage polarization models, we confirmed that lncRNA-MM2P was the lncRNA altered during macrophage M2 polarization. Our data suggest that lncRNA-MM2P might play a role in cytokine-promoted macrophage M2 polarization by maintaining the activation of STAT6. Knockdown of lncRNA-MM2P impaired macrophage polarization and reduced the capacity of macrophages to stimulate angiogenesis both *in vitro* and *in vivo*. Thus, we have shown that lncRNA-MM2P regulates macrophage M2 polarization.

[1]Institute of Pharmacology and Toxicology, Zhejiang Province Key Laboratory of Anti-Cancer Drug Research, College of Pharmaceutical Sciences, Zhejiang University, Hangzhou, China. [2]Affiliated Hangzhou First People's Hospital, Zhejiang University School of Medicine, Hangzhou, China. [3]Tongde Hospital of Zhejiang Province, Hangzhou, China. [4]Department of Orthopedics, The Second Affiliated Hospital of Zhejiang University, Zhejiang University, Hangzhou, China.

Note: Supplementary data for this article are available at Cancer Immunology Research Online (http://cancerimmunolres.aacrjournals.org/).

Corresponding Authors: Bo Yang, Zhejiang University, 866 Yuhangtang Road, Hangzhou, Zhejiang 310058, China. Phone: 86-57188208400; Fax: 86-57188208400; E-mail: yang924@zju.edu.cn; Meidan Ying, Room 115, College of Pharmaceutical Sciences, Zhejiang University, Hangzhou, China. E-mail: mying@zju.edu.cn

doi: 10.1158/2326-6066.CIR-18-0145

Materials and Methods

Reagents

Recombinant murine IL4 and IL13 (210-14 and 200-13) were purchased from PeproTech, Inc. Lipopolysaccharide (LPS, L2880) and sodium orthovanadate (Na_3VO_4, 450243) were purchased from Sigma-Aldrich. Mouse recombinant M-CSF (300-25-50), antibodies against STAT1 (9172s), p-STAT1 (9167s), STAT6 (9362s), p-ERK (9101s), ERK (4695s), p-p38 (9216s), JAK2 (3230s), p-JAK2 (3776s), PU.1 (2266s), and C/EBPβ (3087s) were purchased from Cell Signaling Technology. Antibodies against β-actin (sc1615) and p38 (sc7149) were purchased from Santa Cruz Biotechnology. Antibodies for p-STAT6 (ab54461), CD31 (ab28364), and CD206 (ab64693) were purchased from Abcam. Antibodies for flow cytometry including PE-conjugated anti-mouse CD206 (141706), PE-conjugated anti-mouse CD86 (105008), and FITC-conjugated anti-mouse F4/80 (123108) were purchased from BioLegend. Antibodies against CD209 were purchased from eBioscience (Thermo Fisher Scientific Inc.). The jetPrime transfection agent was obtained from Polyplus (114-15, 850 bd Sébastien Brant 67400 Illkirch FRANCE).

Cell culture

RAW264.7, HUVEC cells, SKOV-3 cells, A2780 cells, K7M2 cells, and KHOS/NP cells were obtained from the Cell Bank of the China Science Academy (Shanghai, China) in 2015. All the cell lines have been tested and authenticated utilizing short tandem repeat profiling every 6 months. RAW264.7, HUVEC, K7M2, KHOS/NP, and A2780 cells were cultured in DMEM, and SKOV-3 cells were cultured in RPMI-1640 medium. All of the media contain 10% FBS and 100U per mL of penicillin–streptomycin. Cells were grown in a 5% CO_2 humidified incubator at 37°C. The cell lines used for experiments had been passaged no more than 20 times and cells were monitored for *mycoplasma* contamination every 6 months.

Bone marrow–derived macrophage (BMDM) isolation and differentiation

BMDMs were produced as previously described with small modification (20). Six-week-old C57BL/6 mice were sacrificed by cervical dislocation and sterilized with 75% ethanol. The skin at the root of hind legs was incised, and muscle tissue was removed with scissors from the bones. Then, the bones were cut from both ends and flushed with medium using a 5-mL syringe. The bone marrow cells blown off were pipetted up and down in a culture dish to be uniform suspension. Bone marrow cells were cultured in DMEM containing 10% FBS and 50 ng/mL M-CSF for 3 days to obtain BMDMs.

Flow cytometry

RAW264.7 and BMDMs were collected with a scraper, blocked with 3% BSA for 45 minutes, and then incubated with PE-conjugated anti-mouse CD86 (1:200), PE-conjugated anti-mouse CD206 (1:200), PE-conjugated anti-mouse CD209 (1:200) or FITC-conjugated anti-mouse F4/80 (1:200), according to the manufacturers' instructions. For each sample, at least 1×10^4 cells were analyzed using the BD FACSCalibur cytometer (Becton Dickinson).

Microarray analysis

RAW264.7 cells and BMDMs were treated with IL13 at the indicated time points. Total RNA from cells of each group was isolated using TRIzol, respectively. RNA expression profiling was performed using the Agilent mouse lncRNA + mRNA microarray V2.0 platform. Quantile normalization and subsequent data processing were performed using Agilent Gene Spring Software 11.5. Heat maps representing differentially regulated genes were generated using Cluster 3.0 software. Microarray data have been deposited in NCBI's Gene-Expression Omnibus database under accession numbers GSE107979 and GSE107952.

Plasmids and cell transfection

The siRNA sequence duplexes were produced by Genepharma, Co. The siRNA sequences used were as follows:

siRNA-lncRNA-MM2P #1: sense: 5′-CACGAAGACUGGAAUGCAATT,

antisense: 5′-UUGCAUUCCAGUCUUCGUGTT;

siRNA-lncRNA-MM2P #2: sense: 5′-GUAGAUGUGUCAAGCGUGUTT,

antisense: ACACGCUUGACACAUCUACTT;

Scramble siRNA: sense: 5′-AUCCGCGCGAUAGUACGUATT,

antisense: 5′-TTUAGGCGCGCUAUCAUGCAU;

The transfection was performed using siRNA and jetPrime according to the manufacturer's recommendations.

To express gene-specific shRNAs under the U6-RNA promoter, sense and antisense oligonucleotides 60 bp in length were ligated into pLKO.1/U6 (Addgene). The sequences of the oligonucleotices were the same as siRNA mentioned above. The resulting plasmids were termed shRNA-MM2P #1 and shRNA-MM2P #2, respectively.

The lentiviral vector pCDH-EF1-Puro plasmid was obtained from System Biosciences and the lncRNA-MM2P (sequence can be found in Supplementary Table S1) was cloned into pCDH plasmid by CloneEZ PCR cloning kit (GenScript) with the following primers: forward-GATTCTAGAGCTAGCGAATTCGTACTGGGAAATGAATCCGG, reverse-ATCCTTCGCGGCCGCGGATCCACATTGTTAAGTTTGTTTATT.

All lentiviral vectors with expression constructs, including shRNA-MM2P #1, shRNA-MM2P #2, and control shRNA, pRD8.9 packaging plasmids, and pMD.G envelope plasmids, were transfected into 293FT cells for packaging. The virus particles were harvested 24 hours after transfection of 293FT cells. For stable transfection, cells were grown in 6-well plates at 50% confluency, and 1 mL of viral supernatant was added with 1 μL polybrene (21).

Quantitative PCR assay

Total RNA from RAW264.7 and BMDMs was extracted from cultured cells using the TRIzol reagent (Invitrogen) according to the manufacturer's instructions. First-strand cDNA was synthesized with Transcript One-Step gDNA Removal and cDNA Synthesis SuperMix (AT311-03, Transgene Biotech Co., Ltd) and analyzed by real-time quantitative PCR with SYBR Premix Ex TaqTMα (RR420A, TaKaRa). The reaction mixtures containing SYBR Green were composed following the manufacturer's protocol. Relative expression of the target genes was normalized to that of the control gene 18s rRNA.

The sequences of the primers used for quantitative real-time-PCR were as follows:

lncRNA-MM2P: forward-TAGCTCCCACGAAGACTGGAAT, reverse-CTATGCTCGTGATTTATAAAACGCAAGTC;

Fizz-1: forward-CCCTGCTGGGATGACTGCTA, reverse-TGCAAGTATCTCCACTCTGGATCT;

PPAR-γ: forward-TTCGATCCGTAGAAGCCGTG, reverse-TTGGCCCTCTGAGATGAGGA;

MRC1: forward-AAGGCTATCCTGGTGGAAGAA, reverse-AGGGAAGGGTCAGTCTGTGTT;

ARG1: forward-AAGAATGGAAGAGTCAGTGTGG, reverse-GGGAGTGTTGATGTCAGTGTG;

YM1: forward-AGACTTGCGTGACTATGAAGC, reverse-ATGAATATCTGACGGTTCTGAGG;

18s rRNA: forward-CGGCTACCACATCCAAGGAA, reverse-GCTGGAATTACCGCGGCT.

Fluorescence *in situ* hybridization (FISH) assay

Cells were fixed for 10 minutes with 4% (w/v) fresh paraformaldehyde in phosphate-buffered saline (PBS) and subsequently washed with PBS. Cells were permeabilized with 0.5% (v/v) Triton X-100 in precooled PBS for 5 minutes and incubated with prehybridization buffer. Before hybridization, the hybridization buffer needed to be at 37°C. Then, the lncRNA, U6 snRNA, and 18S rRNA FISH probes were mixed with hybridization buffer. Prehybridization buffer was aspirated and hybridization mix containing probes was added at 37°C in a humidified incubator overnight. After hybridization, the chamber was washed with 4x SSC (0.6 M NaCl, 0.068 M citric acid, pH 7.0) for several times in the dark. Then incubated with DAPI nuclear stain (5 ng/mL DAPI in PBS) to counterstain the nuclei. The chamber was mounted with an antifade agent. The cells were observed under a confocal microscope (FV1000, Olympus). The lncRNA oligonucleotide probes used for FISH were CY3 labeled. The anti-U6, anti-18S, or anti-lncRNA-MM2P oligodeoxynucleotide probe was designed and synthesized by RiboBio. Prehybridization buffer and hybridization buffer were taken from the Ribo Fluorescent *In Situ* Hybridization Kit (RiboBio).

Conditioned medium preparation

Macrophage polarization was obtained by culturing cells in DMEM medium supplemented with 10% FBS and 10 ng/mL IL4 or IL13 for 2 days. Polarized RAW264.7 cells or BMDMs were incubated in serum-free medium for 24 hours, after which culture supernatants were collected as conditioned medium (CM). CM was centrifuged at 3,000 rpm to remove debris and then stored at −80°C.

Tube formation assay

HUVEC cells (3×10^4 cells per well) were seeded in 96-well plates that were filled with 50 μL Matrigel and solidified at 37°C. The cells were cultured in CM supplemented with 2.5% FBS for 6 hours. To observe the formation of tube-like structures, 5 optical fields (10× magnification) per well were randomly chosen and analyzed by a LEICA DMI 4000B microscope with Leica Application Suite software.

Transwell assay

The cell migration assay was performed in a Transwell Boyden chamber. The cell suspension (2×10^4 cells/mL) was placed in the upper chamber. The lower compartment contained 0.6 mL of CM. After 12- or 24-hour incubation at 37°C, cells were fixed with 75% EtOH and then stained with crystal violet. The stained cells were subsequently photographed.

Western blot analysis

After treatment with reagents for the indicated times, the macrophages were harvested. Cells were resuspended in lysis buffer (50 mmol/L Tris-HCl, 150 mmol/L NaCl, 2 mmol/L EDTA, 2 mmol/L EGTA, 25 mmol/L NaF, 25 mmol/L β-sodium glycerophosphate, 0.3% NP-40, 0.3% Triton X-100, 0.25% Leupeptin, 0.1% PMSF, 0.1% Na_3VO_4). Cell lysates were centrifuged at 13,200 rpm for 30 minutes at 4°C. Proteins were separated in 8% to 12% SDS-PAGE and blotted onto PVDF membranes, then incubated with primary antibodies followed by HRP-labeled secondary antibodies. Protein was detected using an ECL-plus kit and visualized on autoradiography film. Quantity One 1-D analysis software (Bio-Rad) was used for quantification of the Western blot band intensity.

Mice study

BALB/c mice (4–5 weeks old) were obtained from the National Rodent Laboratory Animal Resource (Shanghai, China). All animal experiments were carried out in accordance with the Institutional Animal Use and Care Committee (P-IACUC-003 and P-IACUC-003R).

For the experiment with RAW264.7 cells, mice were randomly chosen and assigned to 3 groups (7 animals per condition). Groups are divided as follows: K7M2 cells + RAW264.7-control, K7M2 cells + RAW264.7-shMM2P #1, K7M2 cells + RAW264.7-shMM2P #2. K7M2 cells (1×10^6) mixed with conditioned macrophages (3×10^6) were implanted subcutaneously into armpits of the mice for 6 weeks. At the termination of the experiment, tumor tissues were harvested and weighted, and the percentage of M2 macrophage were assessed. For the experiment with BMDMs, mice were randomly chosen and assigned to 4 groups (8 animals per condition). Groups are divided as follows: K7M2 only, K7M2 cells + BMDMs-control, K7M2 cells + BMDMs-shMM2P #1, K7M2 cells + BMDMs-shMM2P #2. K7M2 cells (1×10^6) mixed with conditioned BMDMs (6×10^6) were implanted subcutaneously into armpits of the mice for 6 weeks. At the termination of the experiment, tumor tissues were harvested and weighed, and the percentage of M2 macrophage were assessed.

Histology and IHC analysis

Tumor tissues were fixed in 4% PFA for 1 hour, dehydrated overnight at 4°C and then frozen in OCT compound. 8-μm sections from all tissues were cut and stained with hematoxylin and eosin (H&E). All sections were reviewed by a pathologist. Briefly, all steps were performed by the automated instrument according to the manufacturer's instructions in the following order: 30% peroxide block, incubation with mouse monoclonal anti-CD206 (dilution 1:200, ab64693, Abcam), or anti-CD31 (dilution 1:200, ab28364, Abcam), incubation with secondary antibodies (PV-6001, ZSGB-BIO), color development with a DAB detection kit (ZLI-9018, ZSGB-BIO), hematoxylin counterstaining, hydrochloric acid alcohol differentiation, and mounting of the slides.

Statistical analysis

Values are presented as means ± standard deviation (SD). Two-tailed and unpaired Student *t* tests were used for statistical analysis, and differences were considered significant for *P* values less than 0.05.

Results

LncRNA profiling in M2 polarized macrophages

To screen for functional lncRNAs involved in macrophage M2 polarization, we utilized the cellular model of IL13-driven

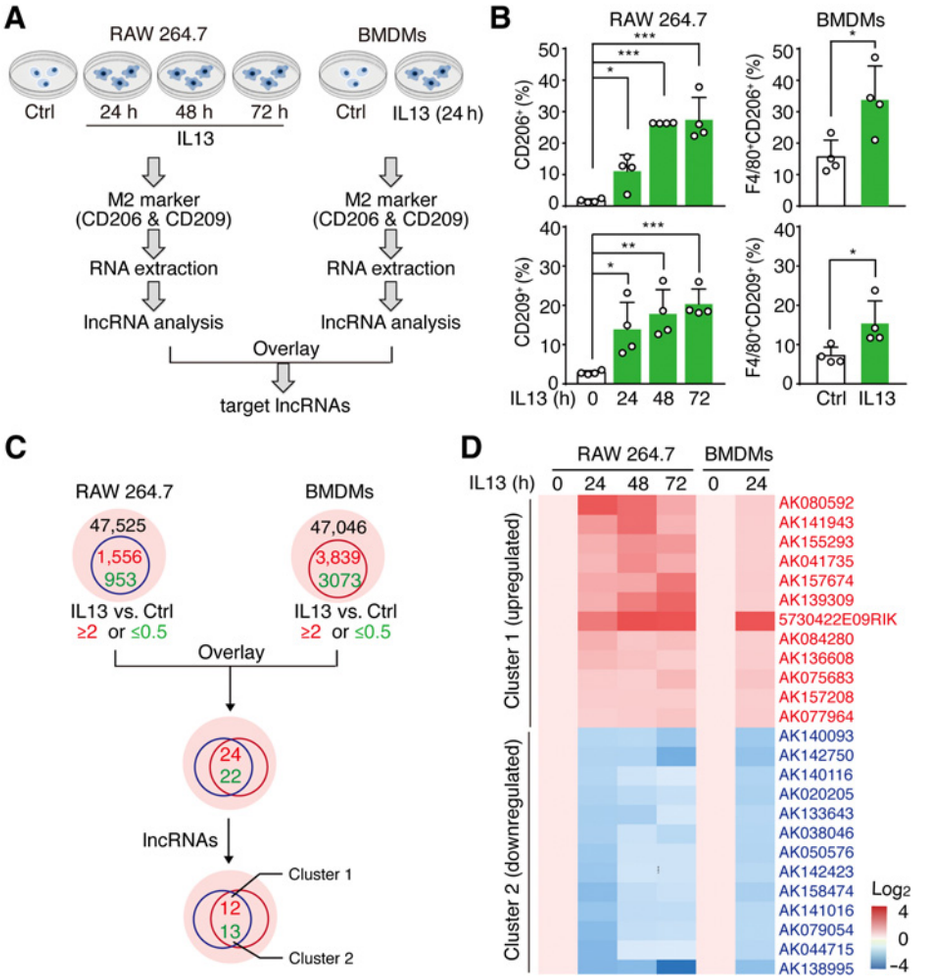

Figure 1.

Expression profiles of lncRNAs in M2 macrophage polarization. **A,** Schematic representation of profiling gene expression in RAW264.7 cells and BMDMs. **B,** RAW264.7 cells or BMDMs were exposed to IL13 (10 ng/mL) for indicated time and harvested for M2 macrophage cell-surface marker (CD206- and CD209-positive expression) analysis by flow cytometry. The statistical data are from four independent experiments, and the bar indicates the SD values (*, $P < 0.05$; **, $P < 0.01$; ***, $P < 0.001$). **C,** Schematic representation of comparing gene-expression profiles in M2-polarized macrophages (2-fold difference, IL13 vs. control) and overlay analysis. **D,** Heat map of 25 lncRNAs correlated with M2 polarization from two macrophage M2 polarization models.

macrophage M2 polarization (22). As shown in Fig. 1A, RAW264.7 cells and mouse BMDM cells were harvested after stimulation with IL13 (10 ng/mL) for the indicated times. To monitor M2 polarization, we assessed the expression of phenotypic markers associated with M2 macrophages, including CD206 and CD209, by flow cytometry (23). As expected, the positive expression rate of the M2-type marker CD206 in RAW264.7 cells was significantly increased after 72 hours of administration of IL13, from 2.62% ± 1.00% to 27.37% ± 3.80%, and the positive expression rate of CD209 was increased from 3.47% ± 0.88% to 20.35% ± 7.14% (Fig. 1B). In line with the results from the RAW264.7 cells, an increase in the proportion of both $F4/80^+$ $CD206^+$ and $F4/80^+$ $CD209^+$ cells was also observed in BMDMs (Fig. 1B). These results confirmed the success of the cellular M2 polarization model we used.

Next, time-course samples of IL13-treated RAW264.7 cells (0, 24, 48, and 72 hours) and BMDM samples (0 and 24 hours) were subjected to lncRNA microarray analysis (Fig. 1A). As shown in Fig. 1C, in RAW264.7 cells, expression of 2,509 genes changed by at least 2-fold (1,556 genes were upregulated and 953 genes were downregulated) after IL13 treatment (Supplementary Table S2). Expression of 6,912 genes changed by at least 2-fold (3,839 genes were upregulated and 3,073 genes were downregulated) during IL13-driven M2 polarization in BMDMs (Fig. 1C; Supplementary Table S3). Among the genes with altered expression, 25 lncRNAs (12 lncRNAs were upregulated and 13 lncRNAs were downregulated) were identified from the two data sets and are shown as heat maps in Fig. 1D (the upregulated lncRNAs were defined as cluster 1, and the downregulated lncRNAs were cluster 2).

LncRNA-MM2P may be involved in M2 macrophage polarization

In order to characterize the lncRNAs involved in the M2 polarization process of macrophages, we further examined the expression of the 25 lncRNAs with altered expression in both IL4-driven M2 macrophage polarization and LPS-driven M1 macrophage polarization cell models (Fig. 2A).

First, we treated RAW264.7 cells with IL4, a cytokine used to induce M2 macrophages. As shown in Supplementary Fig. S1A, IL4 induced an increase of CD206 and CD209 expression, as expected. The expression of 22 lncRNAs showed similar trends as those in the IL13-induced M2 macrophage polarization model (Fig. 1D). Expression of 8 lncRNAs (AK157208, AK075683, AK136608, AK041735, AK155293, AK139309, AK157674, and 5730422E09RIK) changed more than 2-fold during IL4-induced M2 macrophage polarization (Fig. 2B; Supplementary Fig. S1B). Next, we tested the expression of these 25 lncRNAs in the

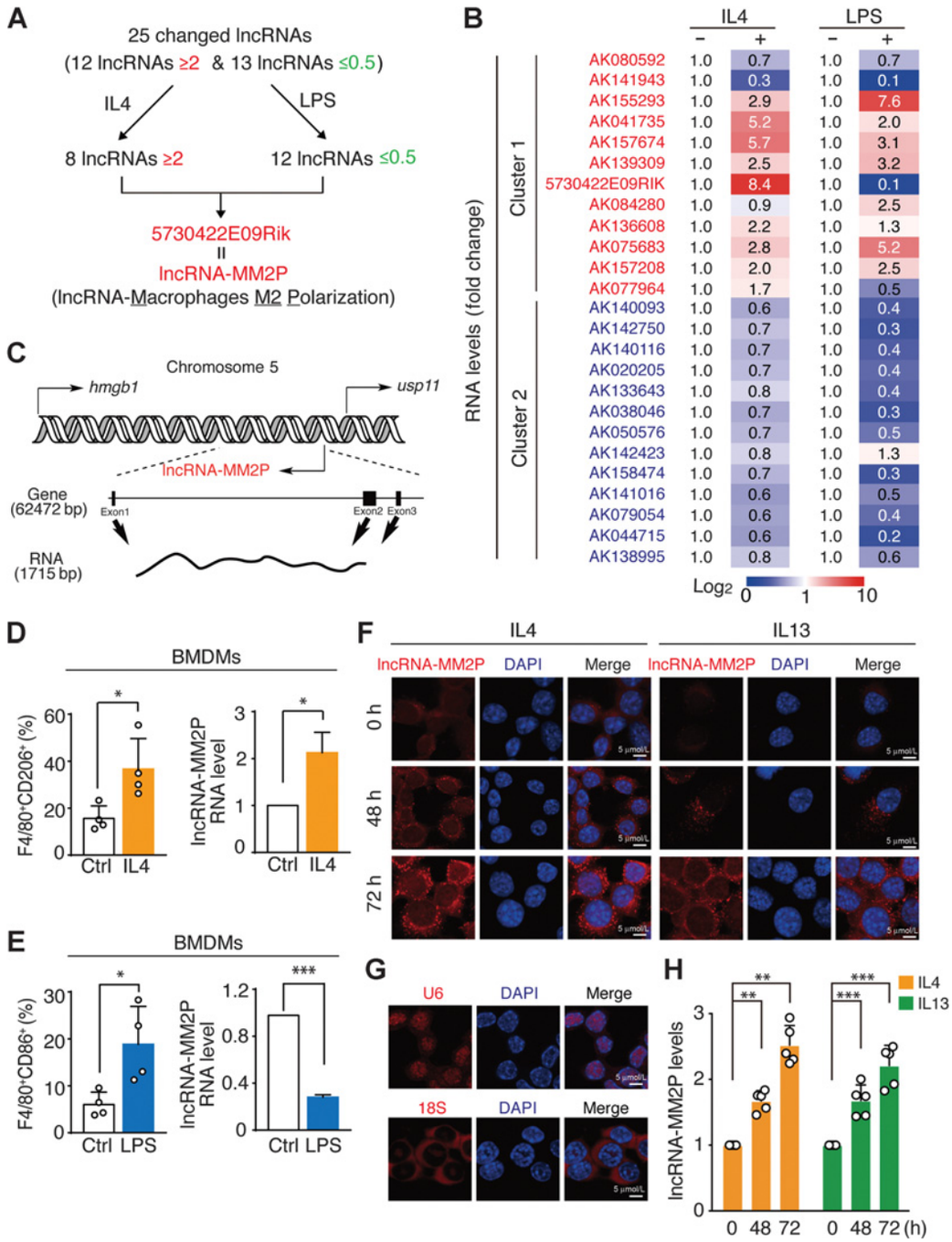

Figure 2.

LncRNA-MM2P is identified as a potential lncRNA involved in M2 macrophage polarization. **A,** Schematic representation of identifying the lncRNAs specifically determined by M2 polarization from 25 potential lncRNAs. Gene expression in RAW264.7 cells and BMDMs. **B,** Validation of expression of 25 lncRNAs in IL4 or LPS-treated RAW264.7 cells by qRT-PCR. RAW264.7 cells were treated with IL4 (10 ng/mL) or LPS (10 ng/mL) for 24 hours, and the relative gene expression is normalized to the control group (without treatment) and the number indicates the mean value from triplicates. **C,** The genomic information of lncRNA-MM2P. **D, E,** BMDMs were treated with IL4 or LPS for 72 hours and flow-cytometric analysis was performed to analyze the percentage of $F4/80^+CD206^+$ or $F4/80^+CD86^+$ cells. BMDMs were treated with IL4 or LPS for 24 hours and the expression of lncRNA-MM2P was analyzed by qRT-PCR. The statistical data are from four independent experiments and the bar indicates the SD values (*, $P < 0.05$; ***, $P < 0.001$). **F,** The FISH assay was conducted to confirm the expression of lncRNA-MM2P. RAW264.7 cells were exposed to IL4 (10 ng/mL) or IL13 (10 ng/mL) for indicated time and test the lncRNA-MM2P expression. The representative images are shown. **G,** The localization of U6 snRNA and 18S rRNA was tested by FISH assay in RAW264.7 cells. **H,** Quantitative analysis of **F**. The statistical data are from five independent experiments and in each experiment at least 20 cells are analyzed. The bar indicates the SD values (**, $P < 0.01$; ***, $P < 0.001$).

LPS-driven M1 polarization model. M1-type marker CD86 was used to confirm M1 polarization (Supplementary Fig. S1C). Expression of 17 lncRNAs (AK044715, AK079054, AK158474, AK050576, AK133643, AK038046, AK020205, AK142750, AK140116, AK140093, AK157208, AK075683, AK041735, AK084280, AK155293, AK139309, and AK157674) changed by more than 2-fold as observed during M2 polarization (Fig. 2B; Supplementary Fig. S1D), suggesting that the changes in the expression of these lncRNAs were associated with the polarization process, regardless of type (M1 or M2).

After merging the data from the three macrophage polarization models, 5730422E09RIK was the only lncRNA upregulated during M2 polarization and downregulated in the M1 macrophages (Fig. 2A and B). Given that the function of 5730422e09Rik has not yet been documented and that the expression spectrum of 5730422E09Rik is determined by M2 polarization, we referred to 5730422E09Rik as lncRNA-MM2P (lncRNA-Macrophages M2 Polarization) in our later experiments (Fig. 2A).

As shown in Fig. 2C, the genomic locus of lncRNA-MM2P is on chromosome 5 between *hmgb1* and *usp11* and is 62,472 base pairs in length. LncRNA-MM2P contains 3 exons, and the transcript is 1,715 base pairs long (Fig. 2C). After searching the NONCODE database (24, 25), we found four noncoding transcripts with homology to lncRNA-MM2P that were more likely to be distributed in immune organs such as the thymus and spleen, and macrophage-enriched tissues such as lung tissue, than in other tissues, suggesting the role of lncRNA-MM2P in immune cells, such as M2 macrophages (Supplementary Fig. S2A and S2B).

To validate the specific expression of lncRNA-MM2P in M2 macrophages, we used BMDMs treated with either IL4 or LPS (26, 27). Again, lncRNA-MM2P was upregulated in IL4-driven M2 polarization and was decreased under the administration of LPS in BMDMs (Fig. 2D and E). Additionally, both fenretinide and all-trans retinoic acid (ATRA), which block macrophage M2 polarization (7, 8), inhibited IL13-induced lncRNA-MM2P expression in RAW264.7 cells (Supplementary Fig. S2C).

To better characterize the expression and subcellular localization of lncRNA-MM2P, we performed a FISH assay. As shown in Fig. 2F–H, both IL4 and IL13 were able to significantly increase the expression of lncRNA-MM2P in RAW264.7 cells. In addition, our data further suggest that lncRNA-MM2P was predominantly localized in the cytosol (Fig. 2F). The U6 snRNA and 18S rRNA were used as controls, as they are localized in the nucleus and cytosol, respectively (Fig. 2G).

Collectively, our data demonstrate that expression of lncRNA-MM2P is dictated by M2 polarization.

LncRNA-MM2P required for IL-induced macrophage M2 polarization

As expression of lncRNA-MM2P is determined by M2 polarization, we asked whether lncRNA-MM2P can affect macrophage M2 polarization. To investigate this possibility, two siRNA sequences were introduced to knock down the expression of lncRNA-MM2P, followed by IL13 or IL4 induction for 72 hours. Quantitative real-time PCR (qRT-PCR) was used to evaluate the knockdown efficacy of the siRNAs. As shown in Fig. 3A, two different lncRNA-MM2P siRNA sequences were able to silence expression of lncRNA-MM2P in both RAW264.7 cells and BMDMs. Flow cytometry results showed that IL13-induced CD206 expression in RAW264.7 cells was significantly decreased after silencing of lncRNA-MM2P (Fig. 3B and C). Similarly, under IL4 stimulation, CD206 expression in RAW264.7 cells was significantly decreased (Fig. 3B and C). Similar trends were also observed in the IL4- and IL13-induced BMDMs M2 polarization cell models (Fig. 3D and E). To confirm our findings, we examined the expression of M2-phenotype marker genes. In line with the flow cytometry results, the qRT-PCR results showed less mRNA for five M2-phenotype markers (*Fizz-1*, *PPAR-γ*, *MRC1*, *ARG1*, and *YM1*) compared with those in the negative control group when lncRNA-MM2P was silenced in both RAW264.7 cells and BMDMs (Fig. 3F; Supplementary Fig. S3A). Additionally, the role of lncRNA-MM2P in macrophage M1 polarization was investigated, and knockdown of lncRNA-MM2P expression was performed followed by LPS induction for 72 hours. No significant difference in the expression of CD86, a marker of macrophage M1 polarization, was found after silencing lncRNA-MM2P in RAW264.7 cells (Supplementary Fig. S3B). Collectively, these data indicate that lncRNA-MM2P is required for IL4- and IL13-induced macrophage M2 polarization.

To test whether lncRNA-MM2P acts in trans, we overexpressed lncRNA-MM2P in RAW264.7 cells (Fig. 3G), followed by IL13 or IL4 treatment. As shown in Fig. 3H and I, overexpression of lncRNA-MM2P significantly increased IL4- and IL13-induced CD206 expression. Even without the interleukin treatment, overexpression of lncRNA-MM2P slightly but significantly increased CD206 expression (Fig. 3I). On the other hand, no significant difference in the expression of CD86 was found in the LPS-triggered M1 polarization cell model after overexpression of lncRNA-MM2P (Supplementary Fig. S3C). These data further suggest that lncRNA-MM2P can act in trans to regulate macrophage M2 polarization.

Angiogenic features of M2 macrophages require lncRNA-MM2P

The next question was whether inhibition of M2 polarization through the inhibition of lncRNA-MM2P could subsequently disturb the biological function of M2 macrophages. First, the effect of lncRNA-MM2P on the migration of tumor cells was evaluated by Transwell assay. RAW264.7 cells or BMDMs were transfected with siRNAs for lncRNA-MM2P, followed by IL13 or IL4 induction for 48 hours. The culture medium was replaced with fresh medium without serum. Then, 24 hours later, the supernatant medium was collected (referred to as CM). To evaluate the impact of the CM on tumor cell migration, three cell lines, SKOV3, A2780, and KHOS/NP, were treated with the CM for 24 hours. As shown in Fig. 4A–D and Supplementary Fig. S4A–S4D, the CM from both IL13- and IL4-treated RAW264.7 cells and BMDMs increased the number of migrated cells in these cell lines. However, no significant difference was found in the lncRNA-MM2P siRNA group compared with the control group (Fig. 4A–D; Supplementary Fig. S4A–S4D).

Next, we evaluated the angiogenesis-promoting effect of lncRNA-MM2P by examining the tube formation of HUVEC. HUVEC cells were seeded in a 96-well plate precoated with Matrigel, then capillary-like structures in the presence of different supernatants of macrophages were counted. As shown in Fig. 4E and F, the CM from both IL13- and IL4- treated RAW264.7 cells significantly increased the number of luminal formations. However, in the lncRNA-MM2P knockdown groups, compared with

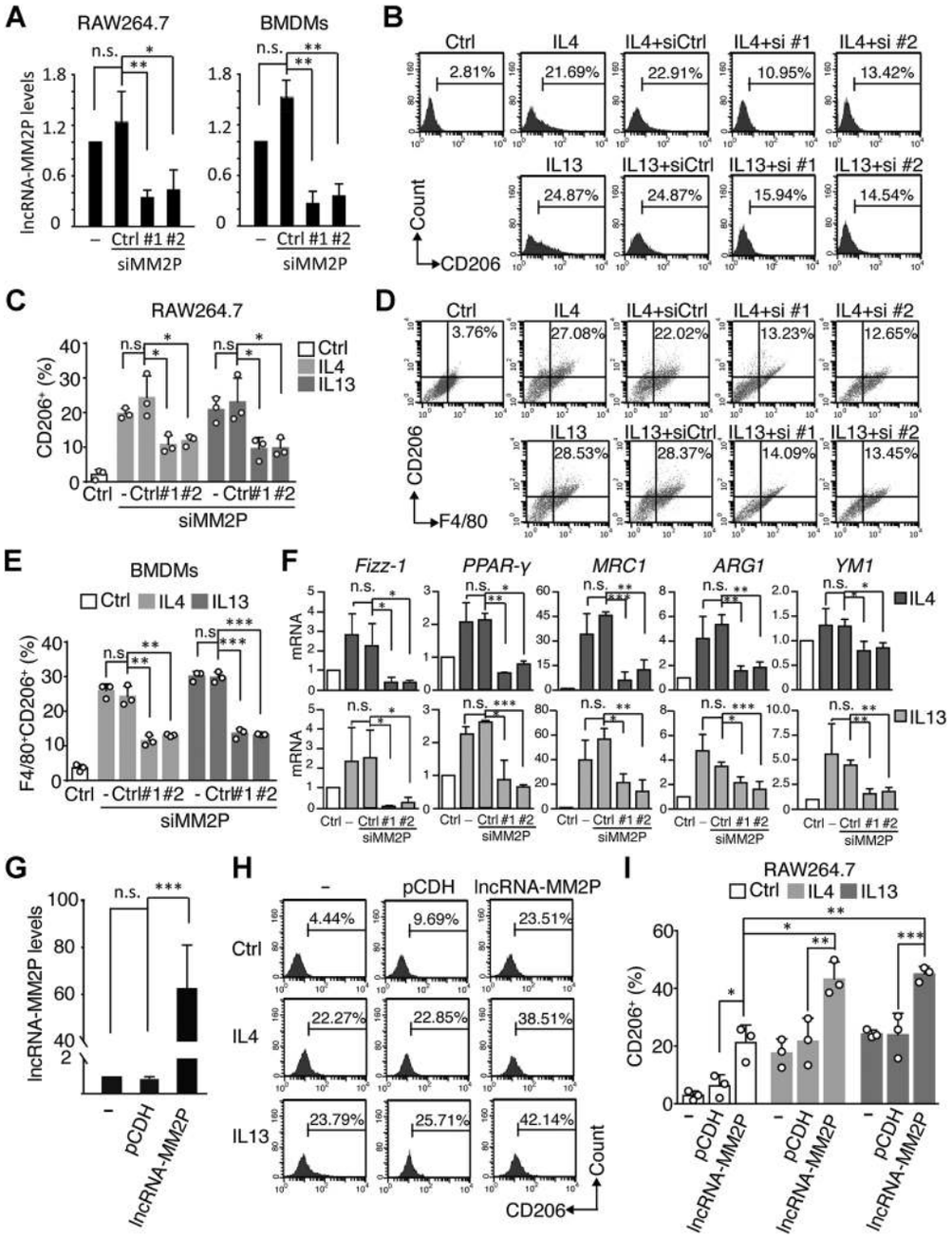

Figure 3.

LncRNA-MM2P mediates macrophage M2 polarization. **A,** The knockdown efficiency of siRNAs against lncRNA-MM2P in RAW264.7 cells and BMDMs was validated by qRT-PCR. The statistical data are from three independent experiments, and the bar indicates the SD values (*, $P < 0.05$; **, $P < 0.01$; n.s., no significant difference). **B** and **C,** RAW264.7 cells were transfected with siRNAs specifically targeting lncRNA-MM2P or control siRNAs for 12 hours and then stimulated with IL13 (10 ng/mL) or IL4 (10 ng/mL) for 72 hours. Flow-cytometric analysis was performed to analyze the percentage of $CD206^+$ cells. The statistical data are from three independent experiments, and the bar indicates the SD values (*, $P < 0.05$, n.s., no significant difference). **D** and **E,** BMDMs were transfected with siRNAs specifically targeting lncRNA-MM2P or control siRNAs for 12 hours and then stimulated with IL13 (10 ng/mL) or IL4 (10 ng/mL) for 72 hours. Flow-cytometric analysis was performed to analyze the percentage of $F4/80^+CD206^+$ cells. The statistical data are from three independent experiments, and the bar indicates the SD values (**, $P < 0.01$; ***, $P < 0.001$; n.s., no significant difference). **F,** mRNA of M2 polarization marker genes in RAW264.7 cells was quantified by qRT-PCR and normalized to 18s rRNA expression. The data are shown as fold change compared with the control group. The statistical data are from three independent experiments and the bar indicates the SD values (*, $P < 0.05$; **, $P < 0.01$; ***, $P < 0.001$; n.s., no significant difference). **G,** The overexpression efficiency of lncRNA-MM2P in RAW264.7 cells was validated by qRT-PCR. The statistical data are from three independent experiments and the bar indicates the SD values (***, $P < 0.001$). **H, I,** Flow-cytometric analysis was performed to analyze the percentage of $CD206^+$ cells after overexpression of lncRNA-MM2P in RAW264.7 cells treated with either IL4 or IL13. The statistical data are from three independent experiments, and the bar indicates the SD values (*, $P < 0.05$; **, $P < 0.01$; ***, $P < 0.001$).

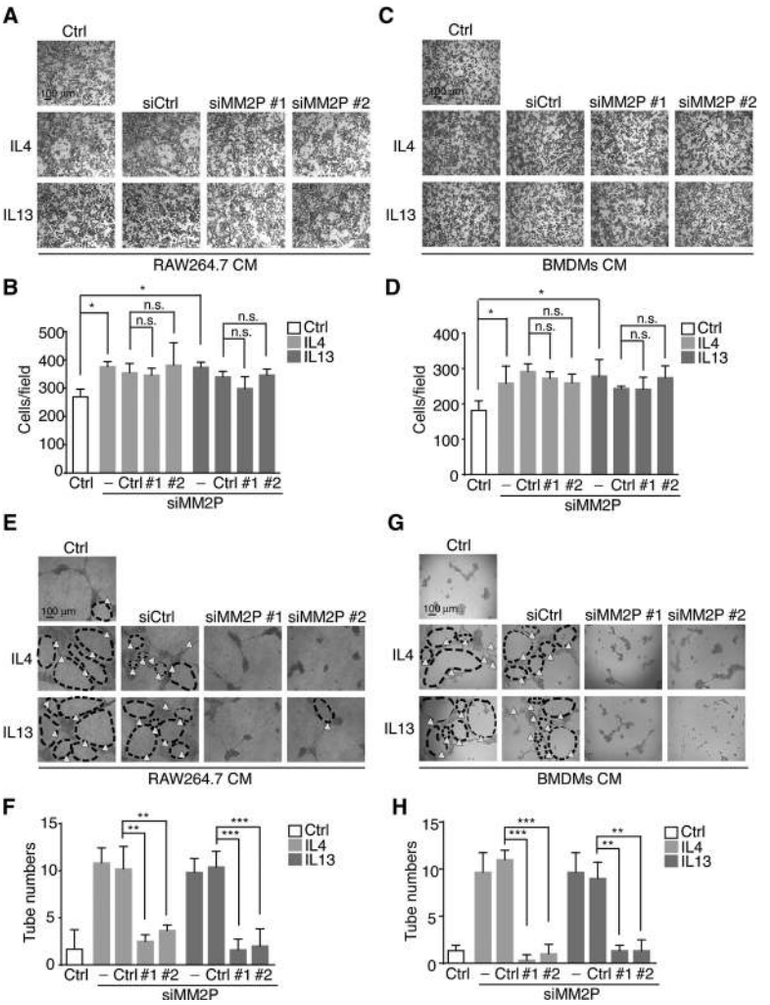

Figure 4.

Knockdown of lncRNA-MM2P eliminates angiogenesis-promoting feature of M2 macrophages. **A–D,** A2780 cells were treated with CM from RAW264.7 cells (**A**) or BMDMs (**C**) for 24 hours and cell migration was assessed by Transwell assay. Representative images are shown, the statistical data are from three independent experiments, and the bar indicates the SD values (*, $P < 0.05$; n.s., no significant difference) (**E–H**) HUVEC cells formed capillary-like structures in the presence of the indicated CM from RAW264.7 cells (**E**) or BMDMs (**G**). The representative images are shown. The statistical data are from three independent experiments, and the bar indicates the SD values (**, $P < 0.01$; ***, $P < 0.001$).

the control group, the number of luminal formations in each field of view significantly decreased (Fig. 4E and F). The effect was observed for the CM from both IL13- and IL4-treated BMDMs (Fig. 4G and H). These results support the idea that knockdown of lncRNA-MM2P affects the angiogenesis-promoting feature of M2 macrophages.

Knockdown of lncRNA-MM2P affects phosphorylation of STAT6

The activation of stimulus-specific transcription factors within the macrophage genome landscape is likely to dictate the functional polarization of macrophages through effects on inducible gene promoters. To gain insight into mechanisms underlying the regulatory role of lncRNA-MM2P, we asked whether lncRNA-MM2P could affect the transcription factors or signaling pathways that regulate M2 polarization of macrophages, such as C/EBPβ, the ERK signaling pathway, and JAK-STAT phosphorylation (11, 28, 29).

RAW264.7 cells were transfected with siRNAs for lncRNA-MM2P, followed by IL13 or IL4 induction for 30 minutes. Knockdown of lncRNA-MM2P did not affect activation of the ERK signaling pathway or the p38 signaling pathway as no significant changes in phosphorylated ERK and phosphorylated p38 were observed after knockdown (Supplementary Fig. S5A and S5B). On the other hand, the knockdown of lncRNA-MM2P did not affect C/EBPβ or PU.1 expression (Supplementary Fig. S5C and S5D), suggesting that the C/EBPβ/PU.1 axis is not involved in lncRNA-MM2P–mediated M2 polarization.

STAT signaling is required to drive M2 macrophage polarization during Th2 cell-mediated immune responses in the presence of IL13 or IL4. As shown in Fig. 5A and B, in RAW264.7 cells, the phosphorylation status of STAT6, but not STAT1, was increased after treating cells with IL13 or IL4 for 30 minutes. The increase in phosphorylated STAT6 was inhibited by knockdown of lncRNA-MM2P, although no difference in phosphorylated STAT1 was observed after knockdown of lncRNA-MM2P (Fig. 5A and B). The effect of lncRNA-MM2P knockdown on STAT6 phosphorylation was also detected in BMDMs (Fig. 5C and D). Our data further suggest that STAT6 might participate in lncRNA-MM2P–mediated polarization of M2 macrophages.

Because our FISH data suggested that lncRNA-MM2P is predominantly localized in the cytosol (Fig. 2F), we were interested in deciphering how lncRNA-MM2P regulates STAT6 phosphorylation. The phosphorylation status of STAT6 is regulated by the upstream kinase JAK2 and by phosphatase. We thus first analyzed

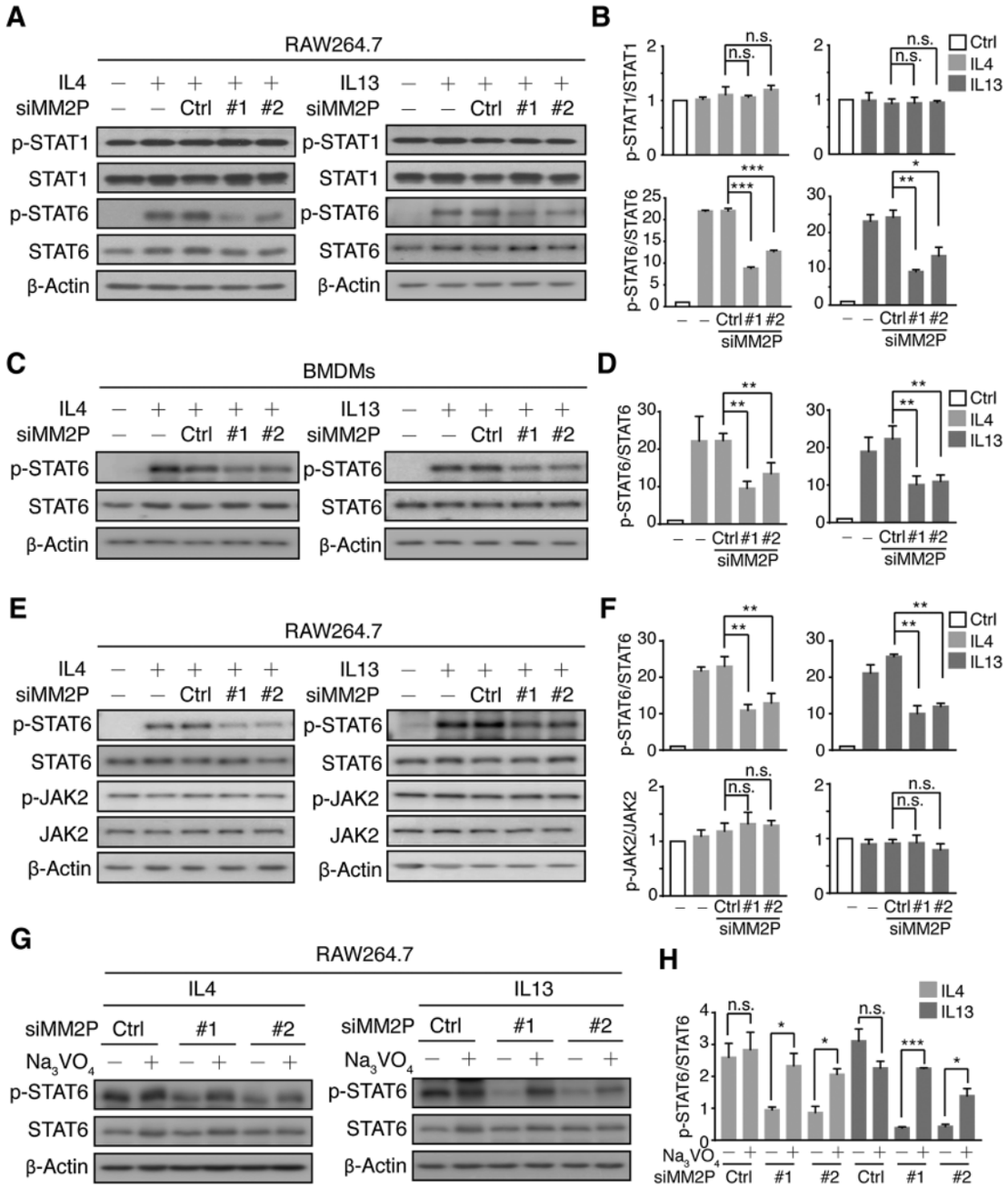

Figure 5.

STAT6 participated in lncRNA-MM2P–mediated M2 macrophage polarization in response to IL13 or IL4. **A,** RAW264.7 cells were transfected with siRNAs specifically targeting lncRNA-MM2P or control siRNAs for 12 hours and then 12 hours later stimulated with IL13 or IL4 for 30 minutes. Western blot detected the expression of p-STAT1, STAT1, p-STAT6, and STAT6 in RAW264.7 cells. **B,** Quantitative analysis of **A**. The statistical data are from three independent experiments and the bar indicates the SD values (*, $P < 0.05$; **, $P < 0.01$; ***, $P < 0.001$; n.s., no significant difference). **C,** BMDMs were transfected with siRNAs specifically targeting lncRNA-MM2P or control siRNAs for 12 hours and then 12 hours later stimulated with IL13 or IL4 for 30 minutes. Western blot detected the expression of p-STAT6, and STAT6 in BMDMs. **D,** Quantitative analysis of **C**. The statistical data are from three independent experiments and the bar indicates the SD values (**, $P < 0.01$). **E,** RAW264.7 cells were transfected with siRNAs specifically targeting lncRNA-MM2P or control siRNAs for 12 hours and then 12 hours later stimulated with IL13 or IL4 for 30 minutes. Western blot detected the expression of p-JAK2, JAK2, p-STAT6, and STAT6 in RAW264.7 cells. **F,** Quantitative analysis of **E**. The statistical data are from three independent experiments and the bar indicates the SD values (**, $P < 0.01$; n.s., no significant difference). **G,** RAW264.7 cells were transfected with siRNAs specifically targeting lncRNA-MM2P or control siRNAs for 12 hours and then 12 hours later treat with 0.5 mmol/L Na_3VO_4 for 10 minutes followed by IL13 or IL4 treatment for another 30 minutes. Western blot detected the expression of p-STAT6, and STAT6 in RAW264.7 cells. **H,** Quantitative analysis of **G**. The statistical data are from three independent experiments, and the bar indicates the SD values (*, $P < 0.05$; ***, $P < 0.001$; n.s., no significant difference).

changes in phosphorylation of JAK2. In RAW264.7 cells, phosphorylated JAK2 could be detected even without IL13 or IL4 treatment, and knockdown of lncRNA-MM2P induced no changes (Fig. 5E and F), suggesting that lncRNA-MM2P might not affect the JAK2-mediated phosphorylation of STAT6. Next, we focused on the dephosphorylation step. By using Na_3VO_4, a tyrosine phosphatase inhibitor, we found that the decrease in p-STAT6 caused by knockdown of lncRNA-MM2P was partially reversed (Fig. 5G and H). Therefore, our data support the idea that the dephosphorylation of STAT6 is regulated by lncRNA-MM2P.

LncRNA-MM2P loss affected M2-driven tumorigenesis and angiogenesis

Given the role of M2 macrophages in promoting tumorigenesis and angiogenesis (8), we investigated the impact of lncRNA-MM2P on functional macrophage–tumor cell cross-talk. RAW264.7 cells infected with shRNA-MM2P #1, shRNA-MM2P #2, or control lentivirus were mixed with K7M2 WT osteosarcoma cells and then implanted subcutaneously into the armpits of mice for 6 weeks. Lentiviral transduction enabled the stable knockdown of lncRNA-MM2P compared with the control virus-transduced cells (Fig. 6A). As expected, the growth of primary tumors after subcutaneous injection of the cell mixture was different between the control group and the lncRNA-MM2P knockdown group (Fig. 6B and C), without differences in the body weight of the mice (Fig. 6D). We found that the vector group was the first to develop tumors (Fig. 6E), which illustrates the positive function of lncRNA-MM2P in tumorigenesis.

To explore whether lncRNA-MM2P played a role in M2 macrophage polarization and angiogenesis, IHC analysis was performed to evaluate the expression of CD206. As shown in Fig. 6F, less CD206 was detected in the tumor region in the lncRNA-MM2P knockdown group than in the control group. Quantitative results were further determined using the log IOD in Image-Pro Plus 6.0, indicating that the amount of CD206 correlated with the tumor growth (Fig. 6G). Because the *in vitro* data suggested that the tumor vessels may also be affected, we further tested whether fewer M2 macrophages would affect vessel numbers in tumor tissues. CD31 staining revealed that tumor vessel numbers were decreased in tumors when lncRNA-MM2P was knocked down (Fig. 6H and I).

To validate these results, we used BMDMs for our mouse study. Indeed, we observed that the addition of BMDMs increased the K7M2 tumorigenesis and tumor growth (Fig. 7A–E). Moreover, knockdown of lncRNA-MM2P affected the BMDMs-promoted K7M2 tumorigenesis and angiogenesis of cancer cells (Fig. 7B–I). Collectively, these observations suggest that lncRNA-MM2P regulates macrophage M2 polarization angiogenesis, and subsequently promotes tumorigenesis and tumor growth.

Discussion

It is believed that the polarization of macrophages is a dynamic process of development and heterogeneity. The phenotypes and functions of macrophages are influenced by the microenvironment (30). LPS induces M1 macrophages (classic activated macrophages), and IL4 or IL13 induces M2 macrophages (alternatively activated macrophages). In the polarization process, transcription factors, which regulate cellular function, undergo changes (31–33). However, the molecular determinants of the control of macrophage plasticity are unknown. Prompted by the progress in genome technology, changes of macrophage transcripts and epigenetics during normal and pathologic conditions have been found to affect macrophages. Determining the factors in macrophage polarization will improve understanding of macrophage regulation in disease.

Although lncRNAs have attracted much attention for their versatile regulatory functions, the role of lncRNAs in macrophage activation has only begun to be appreciated (34–37). This is because the diversity in macrophage phenotypes and functions is subject to genome-wide transcriptional modulations. Thus far, only a few lncRNAs have been reported to be involved in macrophage polarization. Chen and colleagues found that lncRNA-MC acts as a competing endogenous RNA (ceRNA) to modulate monocytopoiesis (34). Huang and colleagues investigated the lncRNAs expression profiles in macrophage polarization in human monocyte–derived macrophages (38). Roux and colleagues identified 204 human and 210 mouse lncRNAs that are differentially expressed following exposure to LPS or IL1β (39). Sun and colleagues demonstrated that lncRNA-GAS5 suppresses transcription of TRF4 to inhibit M2 polarization and exacerbate demyelination (40). In our study, we used cell model-based microarray analysis to profile lncRNAs participating in M2 polarization. Though thousands of lncRNAs were found with greater than 2-fold changes in two cell models, only 25 lncRNAs were altered across different cell lines. Moreover, we found that most of these 25 lncRNAs exhibited the same trends during LPS-triggered M1 polarization, which might suggest that most of these lncRNAs are related to the overall polarization process instead of the specific (M1 or M2) polarization direction. Functional characterization of lncRNA-MM2P generated more insight beyond its identification through high-throughput profiling.

Here, lncRNA-5730422e09Rik was identified as the unique lncRNA specifically upregulated during M2 macrophage polarization from our profiling analysis. LncRNA-5730422e09Rik mediates M2 polarization as well as M2 macrophage-promoted angiogenesis, tumorigenesis, and tumor growth both *in vitro* and *in vivo*. We therefore renamed it lncRNA-MM2P (lncRNA-Macrophage M2 Polarization). The mechanism of action of lncRNAs is complex and has not yet been fully defined. In our study, we found that lncRNA-MM2P affected the phosphorylation of STAT6: the phosphorylation of the tyrosine residue at its Y641 site initiates the transcription of the downstream gene to regulate M2 gene expression in macrophages. Nevertheless, the mechanism of lncRNA-MM2P–regulated STAT6 activation remains elusive. Studies have shown that lnc-DC regulates dendritic cell differentiation and function. Unlike the reported mechanisms for other lncRNAs, lnc-DC promotes STAT3 signaling by interacting with the C-terminus of STAT3 to prevent dephosphorylation of STAT3 Y705 by SHP1 (41). In our experiments, we observed that the dephosphorylation of STAT6 was regulated by lncRNA-MM2P using the phosphatase inhibitor Na_3VO_4. Although there was no evidence to show the mechanism of lncRNA-MM2P, the cytosolic localization of lncRNA-MM2P raises the possibility that interaction between phosphatases such as SHP1 or SHP2 and STAT6 may be a potential mechanism.

In summary, we identified lncRNA-MM2P as a specific regulator of M2 polarization that acts by modulating STAT6

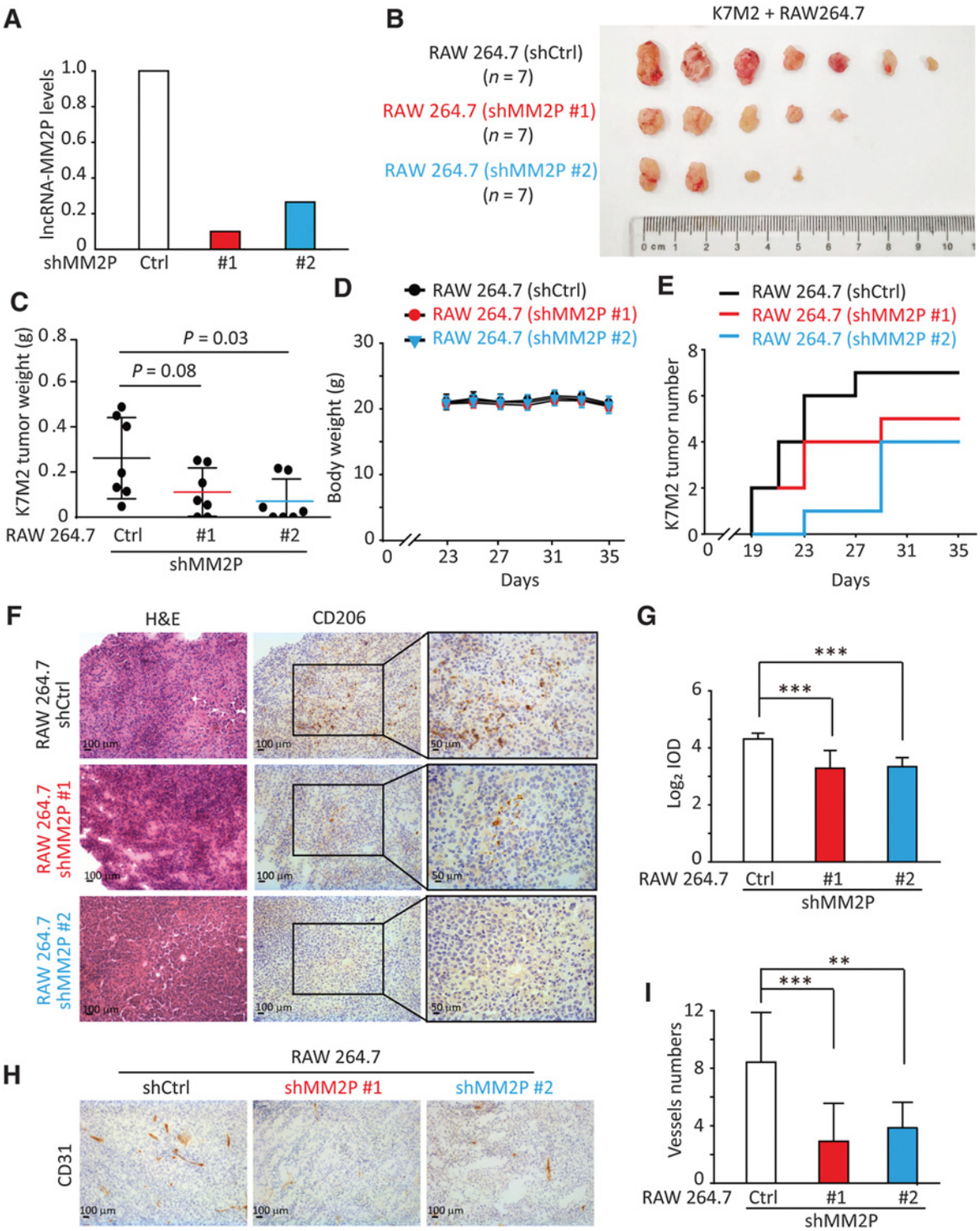

Figure 6.

Knockdown of lncRNA-MM2P impairs RAW264.7 cell–induced tumor growth and angiogenesis of cancer cells. **A,** Expression of lncRNA-MM2P after RAW264.7 cells were infected with shRNA-MM2P lentivirus. The mean value was shown from three experiments. **B** and **C,** The tumors formed in mice at the endpoint of mice study. The statistical analysis of tumor weight in three groups ($n = 7$ per group). **D,** Body weight of each group was measured during the time course. **E,** The tumorigenesis of each group according time course. **F,** Representative histopathologic and IHC image of tumor tissues. M2 macrophages diminished when lncRNA-MM2P was knocked down, as indicated by CD206. **G,** The expression scores of CD206 in the tumor tissues were analyzed by Image-Pro Plus 6.0. **H** and **I,** Representative IHC CD31 stains in tumor borders. Quantification of CD31 positive cells in the tumor tissues. **, $P < 0.01$; ***, $P < 0.001$ ($n = 7$ for the control group, $n = 5$ for shRNA-MM2P #1, and $n = 4$ for shRNA-MM2P #2 in all statistical analysis).

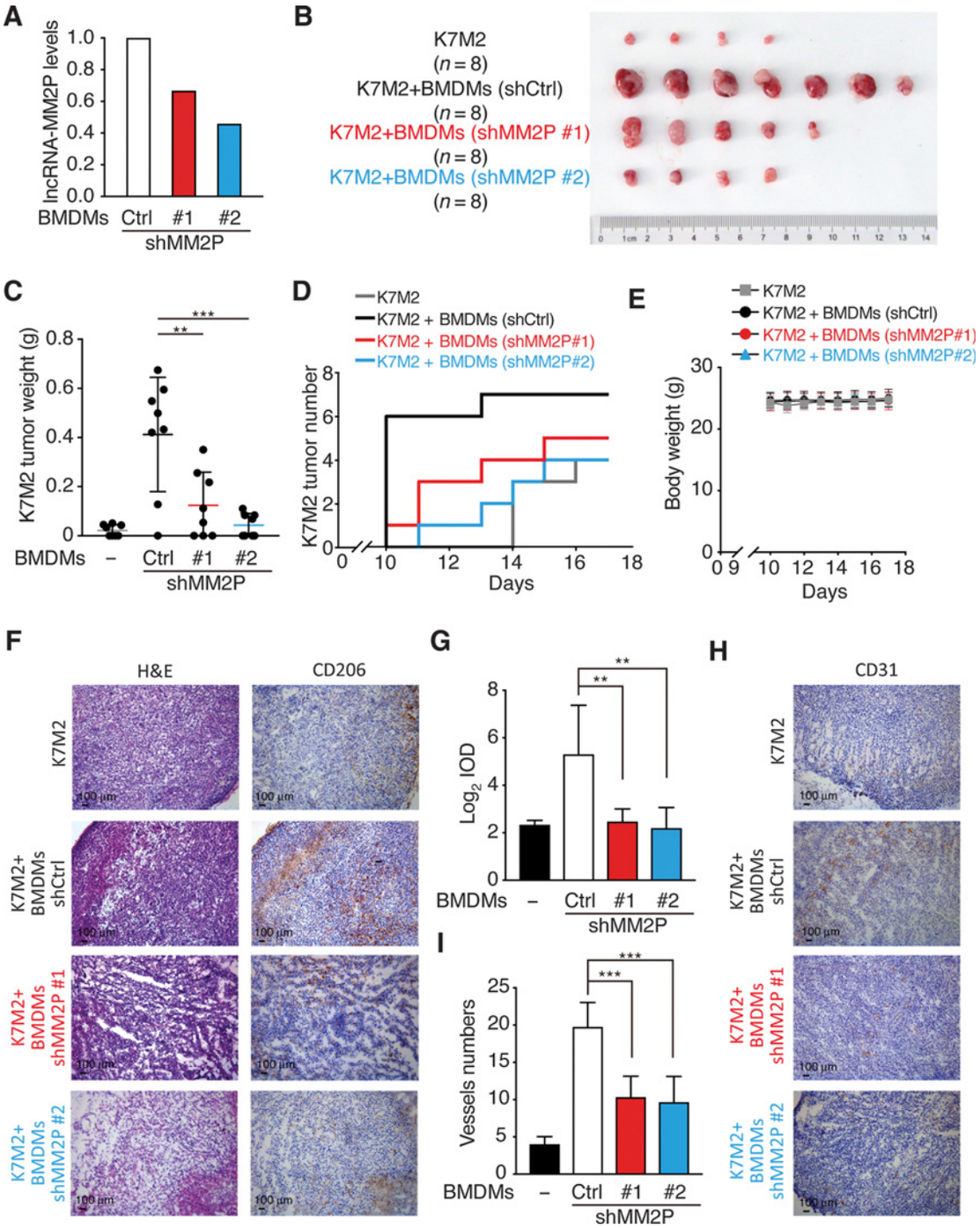

Figure 7.

Knockdown of lncRNA-MM2P impairs BMDM-induced tumor growth and angiogenesis of cancer cells. **A,** Expression of lncRNA-MM2P after BMDMs were infected with shRNA-MM2P lentivirus. **B** and **C,** The tumors formed in mice at the endpoint of mice study. The statistics of tumor weight were analyzed in four groups ($n = 8$ per group). **D,** The tumorigenesis of each group according time course. **E,** Body weight of each group was measured during the time course. **F,** Representative histopathologic and IHC image of tumor tissues. **G,** The expression scores of CD206 in the tumor tissues were analyzed by Image-Pro Plus 6.0. **H** and **I,** Representative IHC CD31 stains in tumor borders. Quantification of CD31 positive cells in the tumor tissues. **, $P < 0.01$; ***, $P < 0.001$ ($n = 4$ for the K7M2-only group, $n = 7$ for control group, $n = 5$ for shRNA-MM2P #1, and $n = 4$ for shRNA-MM2P #2 in all statistical analysis).

phosphorylation. Knockdown of lncRNA-MM2P inhibited macrophage-promoted angiogenesis and impaired tumorigenesis and tumor growth both *in vitro* and *in vivo*. Our work identifies a lncRNA that regulates macrophage M2 polarization and may have relevance to clinical diseases involving M2 macrophage polarization.

Disclosure of Potential Conflicts of Interest

No potential conflicts of interest were disclosed.

Authors' Contributions

Conception and design: J. Cao, M. Ying, B. Yang
Development of methodology: J. Cao, L. Jiang, Y. Gong, Q. Weng
Acquisition of data (provided animals, acquired and managed patients, provided facilities, etc.): J. Cao, R. Dong, L. Jiang, Y. Gong, M. Yuan, J. You, W. Meng, Z. Chen, H. Zhu
Analysis and interpretation of data (e.g., statistical analysis, biostatistics, computational analysis): J. Cao, R. Dong, L. Jiang, M. Yuan, J. You, W. Meng, Z. Chen, H. Zhu
Writing, review, and/or revision of the manuscript: J. Cao, R. Dong, L. Jiang, M. Yuan, J. You, M. Ying, B. Yang
Administrative, technical, or material support (i.e., reporting or organizing data, constructing databases): L. Jiang, M. Yuan, N. Zhang, Q. Weng, H. Zhu
Study supervision: Q. He, M. Ying, B. Yang

Acknowledgments

This work was supported by grants from the National Natural Science Foundation of China (No.81625024 to B. Yang; No.81603126 to N. Zhang; No.81741172 to Q. Weng), Department of Education of Zhejiang Province (Y201430401 to J. Cao), the Zhejiang Provincial Natural Science Foundation (No.LY15H160009 to W. Meng), Medical Science and Technology Planning Project of Zhejiang Province (No.2017201319 to Z. Chen), and the Talent Project of Zhejiang Association for Science and Technology (No.2018YCGC002 to J. Cao).

The costs of publication of this article were defrayed in part by the payment of page charges. This article must therefore be hereby marked *advertisement* in accordance with 18 U.S.C. Section 1734 solely to indicate this fact.

Received March 8, 2018; revised September 1, 2018; accepted November 16, 2018; published first November 20, 2018.

References

1. Yang L, Zhang Y. Tumor-associated macrophages, potential targets for cancer treatment. Biomarker Res 2017;5:25.
2. Allavena P, Sica A, Garlanda C, Mantovani A. The Yin-Yang of tumor-associated macrophages in neoplastic progression and immune surveillance. Immunol Rev 2008;222:155–61.
3. Mantovani A, Locati M. Macrophage metabolism shapes angiogenesis in tumors. Cell Metabolism 2016;24:887–8.
4. Daley D, Mani VR, Mohan N, Akkad N, Ochi A, Heindel DW, et al. Dectin 1 activation on macrophages by galectin 9 promotes pancreatic carcinoma and peritumoral immune tolerance. Nat Med 2017;23:556–67.
5. Guo X, Zhao Y, Yan H, Yang Y, Shen S, Dai X, et al. Single tumor-initiating cells evade immune clearance by recruiting type II macrophages. Genes Develop 2017;31:247–59.
6. Mantovani A, Marchesi F, Malesci A, Laghi L, Allavena P. Tumour-associated macrophages as treatment targets in oncology. Nat Rev Clin Oncol 2017;14:399–416.
7. Zhou Q, Xian M, Xiang S, Xiang D, Shao X, Wang J, et al. All-Trans retinoic acid prevents osteosarcoma metastasis by inhibiting M2 polarization of tumor-associated macrophages. Cancer Immunol Res 2017;5:547–59.
8. Dong R, Gong Y, Meng W, Yuan M, Zhu H, Ying M, et al. The involvement of M2 macrophage polarization inhibition in fenretinide-mediated chemopreventive effects on colon cancer. Cancer Lett 2017;388:43–53.
9. Li X, Yao W, Yuan Y, Chen P, Li B, Li J, et al. Targeting of tumour-infiltrating macrophages via CCL2/CCR2 signalling as a therapeutic strategy against hepatocellular carcinoma. Gut 2017;66:157–67.
10. Sprinzl MF, Puschnik A, Schlitter AM, Schad A, Ackermann K, Esposito I, et al. Sorafenib inhibits macrophage-induced growth of hepatoma cells by interference with insulin-like growth factor-1 secretion. J Hepatol 2015;62:863–70.
11. Lawrence T, Natoli G. Transcriptional regulation of macrophage polarization: enabling diversity with identity. Nat Rev Immunol 2011;11:750–61.
12. Mello SS, Sinow C, Raj N, Mazur PK, Bieging-Rolett K, Broz DK, et al. Neat1 is a p53-inducible lincRNA essential for transformation suppression. Genes Develop 2017;31:1095–108.
13. Durruthy-Durruthy J, Sebastiano V, Wossidlo M, Cepeda D, Cui J, Grow EJ, et al. The primate-specific noncoding RNA HPAT5 regulates pluripotency during human preimplantation development and nuclear reprogramming. Nat Genet 2016;48:44–52.
14. Huarte M. The emerging role of lncRNAs in cancer. Nat Med 2015;21:1253–61.
15. Leung A, Natarajan R. Long noncoding RNAs in diabetes and diabetic complications. Antiox Redox Signal 2018;29:1064–73.
16. Thum T. Noncoding RNAs and myocardial fibrosis. Nat Rev Cardiol 2014;11:655–63.
17. Schonrock N, Harvey RP, Mattick JS. Long noncoding RNAs in cardiac development and pathophysiology. Circ Res 2012;111:1349–62.
18. Sun W, Yang Y, Xu C, Guo J. Regulatory mechanisms of long noncoding RNAs on gene expression in cancers. Cancer Genet 2017;216–217:105–10.
19. Prensner JR, Chinnaiyan AM. The emergence of lncRNAs in cancer biology. Cancer Discov 2011;1:391–407.
20. Weischenfeldt J, Porse B. Bone marrow-derived macrophages (BMM): isolation and applications. CSH Protoc 2008;2008:pdb prot5080.
21. Li Y, Xian M, Yang B, Ying M, He Q. Inhibition of KLF4 by statins reverses adriamycin-induced metastasis and cancer stemness in osteosarcoma cells. Stem Cell Rep 2017;8:1617–29.
22. McWhorter FY, Wang T, Nguyen P, Chung T, Liu WF. Modulation of macrophage phenotype by cell shape. PNAS 2013;110:17253–8.
23. Choi KM, Kashyap PC, Dutta N, Stoltz GJ, Ordog T, Shea Donohue T, et al. CD206-positive M2 macrophages that express heme oxygenase-1 protect against diabetic gastroparesis in mice. Gastroenterology 2010;138:2399–409, 409 e1.
24. Liu C, Bai B, Skogerbo G, Cai L, Deng W, Zhang Y, et al. NONCODE: an integrated knowledge database of non-coding RNAs. Nucleic Acids Res 2005;33:D112–5.
25. Xiyuan L, Dechao B, Liang S, Yang W, Shuangsang F, Hui L, et al. Using the NONCODE database resource. Curr Protoc Bioinform 2017;58:12.16.1–12.16.19.
26. Davis MJ, Tsang TM, Qiu Y, Dayrit JK, Freij JB, Huffnagle GB, et al. Macrophage M1/M2 polarization dynamically adapts to changes in cytokine microenvironments in Cryptococcus neoformans infection. mBio 2013;4:e00264–13.
27. Gocheva V, Wang HW, Gadea BB, Shree T, Hunter KE, Garfall AL, et al. IL-4 induces cathepsin protease activity in tumor-associated macrophages to promote cancer growth and invasion. Genes Develop 2010;24:241–55.
28. Tariq M, Zhang JQ, Liang GK, He QJ, Ding L, Yang B. Gefitinib inhibits M2-like polarization of tumor-associated macrophages in Lewis lung cancer by targeting the STAT6 signaling pathway. Acta Pharmacol Sin 2017;38:1501–11.
29. Binnemars-Postma K, Bansal R, Storm G, Prakash J. Targeting the Stat6 pathway in tumor-associated macrophages reduces tumor growth and metastatic niche formation in breast cancer. FASEB J 2018;32:969–78.
30. Edin S, Wikberg ML, Dahlin AM, Rutegard J, Oberg A, Oldenborg PA, et al. The distribution of macrophages with a M1 or M2 phenotype in relation to prognosis and the molecular characteristics of colorectal cancer. PLoS One 2012;7:e47045.

31. Ben DF, Yu XY, Ji GY, Zheng DY, Lv KY, Ma B, et al. TLR4 mediates lung injury and inflammation in intestinal ischemia-reperfusion. J Surg Res 2012;174:326–33.
32. Kaikkonen MU, Spann NJ, Heinz S, Romanoski CE, Allison KA, Stender JD, et al. Remodeling of the enhancer landscape during macrophage activation is coupled to enhancer transcription. Mol Cell 2013;51:310–25.
33. Quail DF, Bowman RL, Akkari L, Quick ML, Schuhmacher AJ, Huse JT, et al. The tumor microenvironment underlies acquired resistance to CSF-1R inhibition in gliomas. Science 2016;352:aad3018.
34. Chen MT, Lin HS, Shen C, Ma YN, Wang F, Zhao HL, et al. PU.1-Regulated Long noncoding RNA lnc-MC controls human monocyte/macrophage differentiation through interaction with MicroRNA 199a-5p. Mol Cell Biol 2015;35:3212–24.
35. Roy S, Schmeier S, Arner E, Alam T, Parihar SP, Ozturk M, et al. Redefining the transcriptional regulatory dynamics of classically and alternatively activated macrophages by deepCAGE transcriptomics. Nucleic Acids Res 2015;43:6969–82.
36. Sigdel KR, Cheng A, Wang Y, Duan L, Zhang Y. The emerging functions of long noncoding RNA in immune cells: autoimmune diseases. J Immunol Res 2015;2015:848790.
37. Reddy MA, Chen Z, Park JT, Wang M, Lanting L, Zhang Q, et al. Regulation of inflammatory phenotype in macrophages by a diabetes-induced long noncoding RNA. Diabetes 2014;63:4249–61.
38. Huang Z, Luo Q, Yao F, Qing C, Ye J, Deng Y, et al. Identification of differentially expressed long non-coding RNAs in polarized macrophages. Sci Rep 2016;6:19705.
39. Roux BT, Heward JA, Donnelly LE, Jones SW, Lindsay MA. Catalog of differentially expressed long non-coding RNA following activation of human and mouse innate immune response. Front Immunol 2017;8:1038.
40. Sun D, Yu Z, Fang X, Liu M, Pu Y, Shao Q, et al. LncRNA GAS5 inhibits microglial M2 polarization and exacerbates demyelination. Embo Rep 2017;18:1801–16.
41. Wang P, Xue Y, Han Y, Lin L, Wu C, Xu S, et al. The STAT3-binding long noncoding RNA lnc-DC controls human dendritic cell differentiation. Science 2014;344:310–3.